

Optical and Dispersion Parameters of the Al-doped ZnO Thin Film

A.I. Kashuba^{1,*}, B. Andriyevsky², H.A. Ilchuk¹, R.Yu. Petrus¹, T.S. Malyi³, I.V. Semkiv¹

¹ Lviv Polytechnic National University, 12, S. Bandera St., 79646 Lviv, Ukraine

² Faculty of Electronics and Computer Sciences, Koszalin University of Technology, 75-453 Koszalin, Poland

³ Ivan Franko National University of Lviv, 8, Kyrylo and Mefodiy St., 79005 Lviv, Ukraine

(Received 09 March 2021; revised manuscript received 06 August 2021; published online 20 August 2021)

The results of studies of the dispersion of optical functions and optical constants for zinc oxide thin film doped with aluminum are presented. The deposition of Al-doped ZnO (2.5 wt. %) thin films is performed by magnetron sputtering. Al-doped ZnO thin film crystallizes in a hexagonal structure (structure type ZnO, space group $P6_3mc$ (No. 186) with unit-cell dimensions $a = 3.226(2)$ Å and $c = 5.155(6)$ Å ($V^{\circ} = 46.49(6)$ Å³). Optical transmittance spectra (300-2500 nm) shows that the Al-doped ZnO thin film is of high optical quality, and the value of the optical band gap (3.26 eV) is very close to undoped samples. The study of optical functions is performed on the basis of the experimentally measured transmission spectrum using the bypass method. The spectral behavior of optical functions, such as refractive index, extinction coefficient, absorption index, dielectric functions and optical conductivity, is established. The value of Urbach energy and the dependence of oscillator strength on the size of the band gap and the concentration of doping element are determined. It is observed an increase in Urbach energy for the Al-doped ZnO thin film in comparison to the undoped ones. An almost twofold increase in the optical oscillator strength value is revealed for the thin film studied. The influence of aluminum doping on the dynamic change of optical mobility, optical resistance and relaxation time is established for the first time for the studied compound. The value of the plasma frequency is also determined and its correlation with the carrier density is defined. The doping of ZnO thin films with aluminum leads to an increase in optical mobility, relaxation time and plasma frequency that is revealed by comparison with reference data for the undoped ZnO. Due to good optical properties, this thin film is a good candidate as a material for optoelectronic devices.

Keywords: Thin films, Absorption, Dispersion, Refractive index, Transmission, Optical function, Relaxation time.

DOI: [10.21272/jnep.13\(4\).04006](https://doi.org/10.21272/jnep.13(4).04006)

PACS numbers: 78.20. - e, 78.20.Ci, 78.55.Et

1. INTRODUCTION

ZnO thin films attract considerable attention of researchers as a promising material for solar energy, gas sensors and other applications [1-7]. In the classical case, zinc oxide is a wide band gap semiconductor with high exciton binding energy of 60 meV [8].

It is known that optical properties of semiconductor thin films depend on the deposition method [9, 10]. Currently, various methods are used to obtain ZnO thin films: radio frequency (RF) or direct current sputtering, spray pyrolysis, spin coating, metal organic chemical vapor deposition and pulsed laser deposition [5-7, 9-19].

ZnO is usually doped with different chemical elements to modify the optical transmittance and band gap of the corresponding thin films by changing their electrical, optical and other properties. Degree of Al-doping plays a major role in increasing the optical band gap of ZnO thin films and the enhancement of their optical transparency.

Doping of zinc oxide thin films results in different changes of physical properties. In most cases, doping of thin films results in an increase in the band gap value [11-13, 15-22] caused by the influence of the Burstein-Moss effect [20-22] and increased contribution of defects [21] (Zn, O vacancies). In several studies [23-26], doping with different chemical elements leads to a decrease in the band gap, or the value of the band gap remains almost independent of doping.

As a consequence, the physical properties of zinc oxide

thin films may depend on the deposition method or the alloying chemical element. Since one of the predominant applications of zinc oxide thin films is solar energy (ZnO as a conductive material) and gas sensors, it is important to know the behavior of optical functions and optical constants (including optical mobility, relaxation time and optical resistance).

Aluminum (2.5 wt. %) as the doping element and RF sputtering as the preparing method were chosen in the present study. Currently, no reference data on the main optical parameters (optical mobility, relaxation time, optical resistance) of ZnO:Al thin films obtained by RF sputtering are available.

2. EXPERIMENTAL DETAILS

Al-doped ZnO (ZnO:Al) thin films were deposited on glass substrates with a size of $16 \times 8 \times 1.1$ mm³ by the method of high-frequency (HF) magnetron sputtering (~ 13.6 MHz) using a VUP-5M vacuum station (Selmi, Ukraine) [9, 27]. As a target the disc from sintered ZnO (purity of 99.99 %) powder with Al₂O₃ (2.5 wt.%) admixture was used. The target-substrate distance was 60 mm. The start and end of the process were controlled by means of a movable shutter.

The power of the HF magnetron was maintained at a level of 30 W, and the substrate temperature was 373 K. A high-temperature tungsten heater with a power of 300 W was used to heat the substrates. The temperature was controlled by means of a proportional-

* AndriyKashuba07@gmail.com

integral-derivative (PID) controller for controlling heating and cooling rates, as well as for ensuring the temperature conditions of deposition.

Spectral dependences of the optical transmittance (Shimadzu UV-3600) of the title samples have been measured in the visible and near infrared regions (300-2500 nm) at room temperature [9, 27].

3. RESULTS AND DISCUSSION

3.1 The Optical Band Gap E_g and Urbach Parameter E_0

The transmittance spectrum of ZnO:Al thin films is given in Fig. 1. As-grown thin films are found to exhibit high transparency in the wavelength range 300-2500 nm. Here, the average transmittance is close to 78 %.

To determine the thickness of the films under investigation, we can use the following equation:

$$d = \frac{M \cdot \lambda_1 \cdot \lambda_2}{2(n(\lambda_1) \cdot \lambda_2 - n(\lambda_2) \cdot \lambda_1)}, \quad (1)$$

where λ_1 and λ_2 are the wavelengths corresponding to the neighboring extreme points in the transmission spectrum, $M = 1$ for two neighboring extrema of one type (max-max, min-min) and $M = 0.5$ for two neighboring extrema of opposite types (max-min, min-max). The thickness of ZnO:Al thin films calculated by Eq. (1) is equal to 455 nm.

To estimate the absorption band edge energy of the films, the first derivative of the optical transmittance can be used. The dependence of $dT/d\lambda$ versus wavelength λ is plotted, as shown in the inset of Fig. 1. Position of the characteristic highest first peak of $dT/d\lambda$ corresponds to the optical band gap energy $E_g = 3.22$ eV.

The optical band gap E_g is also determined from the spectrum of the absorption coefficient $\alpha(h\nu)$. For this purpose, the known Tauc relation for the direct optical transition between the valence and conduction bands is used [9, 27],

$$(\alpha h\nu)^2 = A(h\nu - E_g), \quad (2)$$

where A is an energy-independent constant and $h\nu$ is the photon energy. Here, the absorption spectrum $\alpha(h\nu)$ is calculated from the transmittance data in the spectral range of stronger absorption [28]. The direct optical band gap E_g is obtained by plotting the dependence of $(\alpha h\nu)^2$ versus $h\nu$ and following linear approximation of this dependence to the value $(\alpha h\nu)^2 = 0$ (Fig. 2). Thus, we have evaluated the exact value of the direct optical band gap for the films studied equal to $E_g^{(d)} = 3.26$ eV. The estimated band gap values of the studied ZnO:Al films obtained by two above mentioned methods are presented in Table 1.

The spectral dependence $\alpha(h\nu)$ near the band edge reveals an exponential dependence on the photon energy and obeys Urbach empirical formula (3),

$$\alpha(h\nu) = \alpha_0 \exp\left(\frac{h\nu}{E_u}\right), \quad (3)$$

where α_0 and E_u (Urbach energy) are the characteristic parameters of the material studied. One can determine

the parameters α and E_u from the experimental dependence $\alpha(h\nu)$ (Fig. 3). The value of Urbach energy E_u depends on the structural disorder and temperature of the material. Temperature dependence of this energy is formed by the interaction of electrons/excitons with optical phonons [24].

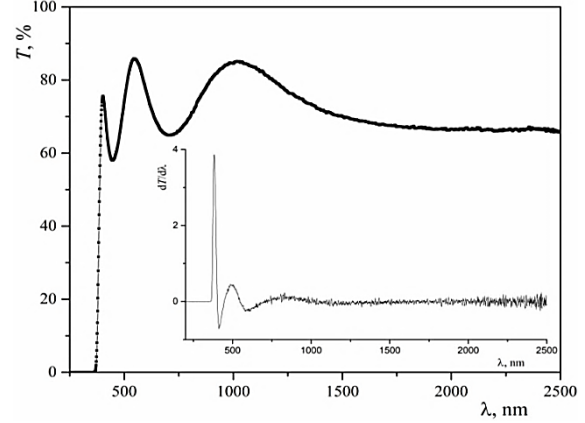


Fig. 1 – Transmission spectrum of ZnO:Al thin film. Plot of the transmittance first derivative $dT/d\lambda$ vs. λ of ZnO:Al thin film

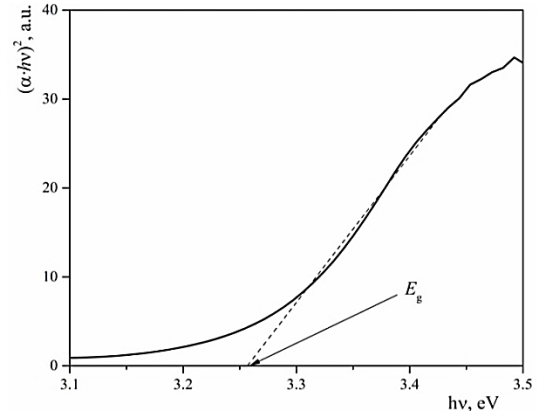


Fig. 2 – Plots of $(\alpha h\nu)^2$ vs. photon energy of ZnO:Al thin film

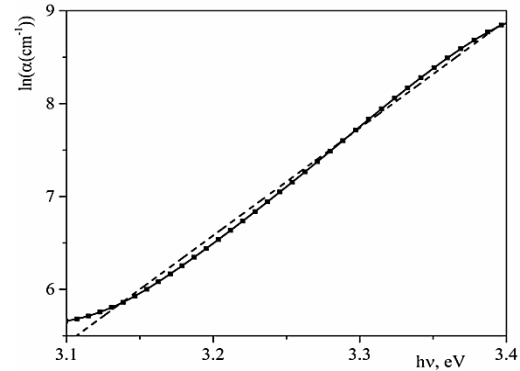


Fig. 3 – Urbach plots of ZnO:Al thin film

It is found that Urbach energy of ZnO:Al films studied increases with increasing doping of zinc oxide by aluminum (Table 1) that may be caused by an increase in the energy width of localized energy states of thin films. However, a more elaborated theory of the experimentally observed exponential dependence $\alpha(h\nu)$ is still absent. This dependence may arise from the random fluctuations of the internal fields associated

with structural disorder in many amorphous materials. The exponential dependence of the optical absorption coefficient with photon energy may arise from the electronic transitions between localized states [29]. In

many cases, the density of the top valence and bottom conduction band states of materials depend exponentially on the energy in the band gap region that is consistent with Tauc theory.

Table 1 – Optical parameters of ZnO and ZnO:X (X = Al, Cu, In, Sn, Mn, Mg, Ni, NiO and Fe-Ni) thin films

Sample	Method of deposition	d , nm	T_{ave} , %	E_g , eV	$E_g(dT/d\lambda)$, eV	E_u , meV	Ref.
ZnO:Al (2.5 wt.%)	RF	455	77.78	3.26	3.22	86.32	This work
ZnO:Al	Spray Pyrolysis	–	≥ 80 %	3.30	–	91	[15]
ZnO:Cu	Spray Pyrolysis	–	≥ 70 %	3.27	–	98	[15]
ZnO:Sn	Spray Pyrolysis	–	≥ 80 %	3.28	–	101	[15]
ZnO	Sol-Gel	–	~ 90	3.29	–	367	[24]
ZnO:In (1.0 %)	Sol-Gel	–	~ 90	3.26	–	390	[24]
ZnO	Coating	–	≥ 80 %	3.288	–	–	[23]
ZnO:Fe-Ni (2 %)	Coating	–	≥ 80 %	3.258	–	–	[23]
ZnO (1:1)	Sol-Gel spin coating method	–	≥ 85 %	3.37	3.31	–	[30]
ZnO (0 kGy)	RF	134	–	3.26	–	116.71	[14]
ZnO	Spray Pyrolysis	210	–	3	–	~ 730	[13]
ZnO:Sn (4 at.%)	Spray Pyrolysis	223	–	3.25	–	~ 200	[13]
ZnO:Mn (4 at.%)	Spray Pyrolysis	192	–	3.17	–	~ 210	[13]
ZnO:Al (4 at.%)	Spray Pyrolysis	178	–	3.08	–	~ 400	[13]
ZnO	Sol-Gel	–	~ 85 %	3.36	–	255	[16]
ZnO:Mg (6 wt.%)	Sol-Gel	–	~ 85 %	3.73	–	307	[16]
ZnO	Spray pneumatic method	149.65	~ 80 %	3.26	–	92	[18]
ZnO:NiO (3 %)	Spray pneumatic method	101.4	~ 80 %	3.28	–	91	[18]
ZnO	Spray Pyrolysis	~ 400	60-70 %	~ 3.27	–	23.34	[19]
ZnO:Ni (5 at.%)	Spray Pyrolysis	~ 400	60-70 %	~ 3.27	–	~ 120	[19]

3.2 Analysis of the Refractive Index

The dispersions of the refractive index $n(\lambda)$ and extinction coefficient $k(\lambda)$ ($k(\lambda) = \lambda\alpha(\lambda)/4\pi$) (Fig. 4) of a thin film can be easily evaluated from the transmission spectrum with interference effects using the envelope method [9, 31-32]. This method is applicable in the case of a weakly absorbing thin film on an entirely transparent substrate, which is much thicker than a thin film. These conditions are met in this work.

The calculated refractive index n of the thin film studied decreases with increasing wavelength λ (see Fig. 4). Here, the dispersion $n(\lambda)$ is normal and may be well approximated by the single oscillator model. In Fig. 5 and Fig. 6, the dashed straight lines are the linear fits of the refractive index dispersions corresponding to the single oscillator model in the form proposed by Wemple and DiDomenico [9],

$$n(h\nu)^2 - 1 \cong \frac{E_d \cdot E_0}{E_0^2 - (h\nu)^2}, \quad (4)$$

where E_0 is the single oscillator energy, E_d is the dispersion energy, and $h\nu$ is the photon energy. Both Wemple parameters, E_0 and E_d , can be obtained from the parameters of the above-mentioned linear fit $(n^2 - 1)^{-1} \sim (h\nu)^2$ of the dependence (4). The values of these parameters are summarized in Table 2. The refractive index $n_0 = n(h\nu = 0)$ can be determined by

using the expression $n_0 = \sqrt{1 + \frac{E_d}{E_0}}$. The value n_0 usually

increases with doping of ZnO by aluminum (Table 2) that may be considered together with the characteristic dimensions of Al atoms in the ZnO structure [33].

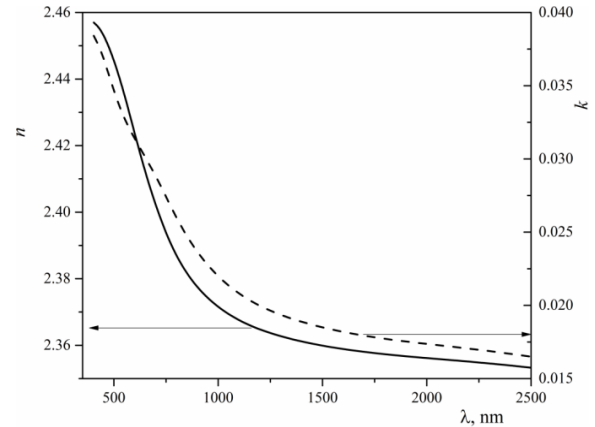


Fig. 4 – Refractive index (left) and extinction coefficient (right) depending on wavelength of ZnO:Al thin film

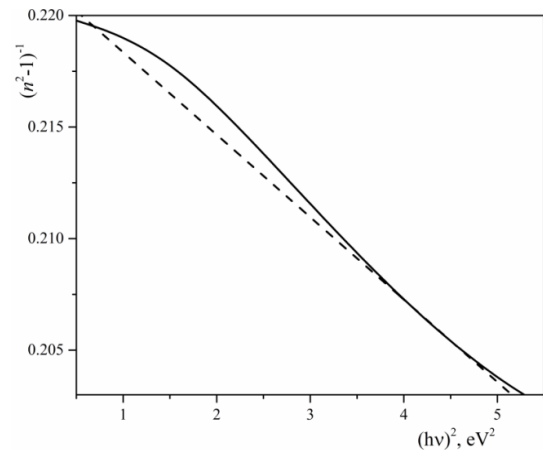


Fig. 5 – Plot of $(n^2 - 1)^{-1} \sim (h\nu)^2$ for ZnO:Al thin film

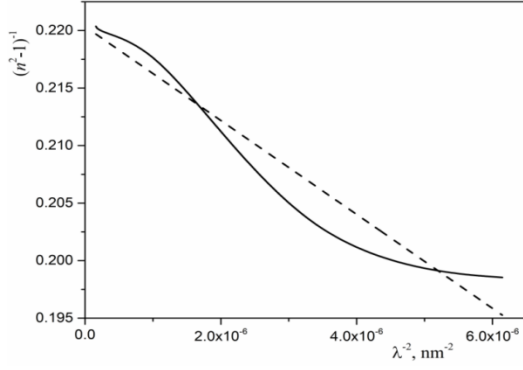


Fig. 6 – Plot of $(n^2 - 1)^{-1} \sim$ vs. λ^{-2} for ZnO:Al thin film

The M_{-1} and M_{-3} moments of the optical spectra can be obtained from the following relations [29]:

$$E_0^2 = \frac{M_{-1}}{M_{-3}}, E_d^2 = \frac{M_{-1}^3}{M_{-3}}. \quad (5)$$

The obtained values are given in Table 2. In addition, the oscillator strength (f) is expressed according to Wemple and DiDomenico via the following formula [24]:

Table 2 – Single oscillator parameters of ZnO:Al thin films

Sample	Method of deposition	E_0 , eV	E_d , eV	n_0	M_{-1}	M_{-3} , eV $^{-2}$	f	λ_0 , nm	S_0 , nm $^{-2}$	Ref.
ZnO:Al (2.5 wt. %)	RF	4.48	20.24	2.35	4.52	0.23	90.68	136.1	$2.5 \cdot 10^{-4}$	This work
ZnO	Sol-Gel	6.62	5.36	1.35	0.89	0.020	35.48	285	$1.06 \cdot 10^{-5}$	[24]
ZnO:In (1.0 %)	Sol-Gel	6.80	8.56	1.50	0.81	0.017	58.20	305	$1.34 \cdot 10^{-5}$	[24]

3.3 The Complex Dielectric Function

It is known that the real and imaginary parts, ε_1 and ε_2 , of the complex dielectric permittivity ε ,

$$\varepsilon = \varepsilon_1 + i\varepsilon_2, \quad (8)$$

are related to the refractive index n and extinction coefficient k by Eqs. (9) and (10),

$$\varepsilon_1 = n^2 - k^2, \quad (9)$$

$$\varepsilon_2 = 2nk. \quad (10)$$

For the values of n much greater than k , the value of ε_1 is approximately equal to n^2 , and the dependence of $\varepsilon_1(\lambda)$ can be fitted using the relation [9] valid for the free electron light absorption,

$$\varepsilon_1 = n^2 = \varepsilon_\infty - \left(\frac{e^2}{\pi c^2} \right) \left(\frac{N_c}{m^*} \right) \lambda^2, \quad (11)$$

where c is the speed of light, m^* is the effective mass of the carrier, N_c is the carrier density, e is the electronic charge, and ε_∞ is the high-frequency dielectric constant. To obtain the high frequency dielectric constant ε_∞ , we plot a graph n^2 as a function of λ^2 and extrapolate the linear part of the curve to $\lambda^2 = 0$ (Fig. 7).

Furthermore, the dispersion of the imaginary part of the dielectric function $\varepsilon_2(\lambda)$ is used to estimate the

$$f = E_0 E_d. \quad (6)$$

Aluminium doping of ZnO film (ZnO:Al, 2.5 wt.%) leads to an increase in the oscillator strength value from 35.48 (ZnO [24]) to 90.68 eV 2 (Table 2). Similar fluctuations of the oscillator strength for the doped thin films were observed in other studies [29], but there is no clear understanding of such behavior of the oscillator strength till now.

The refractive index dispersion $n(\lambda)$ in the range of transparency can be approximated also by using Sellmeier dispersion Eq. (7),

$$(n^2 - 1)^{-1} = \frac{1 - \left(\frac{\lambda_0}{\lambda} \right)^2}{S_0 \lambda_0^2}, \quad (7)$$

where S_0 is the average oscillator strength and λ_0 is the average interband oscillator wavelength. When the dependence of $(n^2 - 1)^{-1}$ vs. λ^{-2} is plotted and the straight-line fit is performed, then the values of S_0 and λ_0 can be determined from the relation (7) (Table 2).

relaxation time (τ), optical mobility (μ_{opt}) and optical resistivity (ρ_{opt}) in the framework of the Drude free electron model [23, 34] using the relation

$$\varepsilon_2 = \left(\frac{e^2}{4\varepsilon_0 \pi^3 c^3} \right) \left(\frac{N_c}{m^*} \right) \left(\frac{1}{\tau} \right) \lambda^3. \quad (12)$$

The parameter τ is found from the slope of the plot $\varepsilon_2(\lambda^3)$, where the value of N_c/m^* is taken from Eq. (11). Afterwards, the optical mobility μ_{opt} and optical resistivity ρ_{opt} of ZnO:Al thin films are calculated by the relations (13) and (14) [34],

$$\mu_{opt} = \frac{e\tau}{m^*}, \quad (13)$$

$$\rho_{opt} = \frac{1}{e\mu_{opt}N_c}. \quad (14)$$

The calculated values of the relaxation time τ , optical mobility μ_{opt} and optical resistivity ρ_{opt} are presented in Table 3.

It is found that the aluminium doping of ZnO thin films increases the values of optical mobility and relaxation time (Table 3). In addition, it is revealed that 2.5 wt. % doping of ZnO by aluminium leads to higher values of optical mobility and relaxation time than those for ZnO thin films doped with Fe-Ni [23].

Additionally, the electron plasma frequency (ω_p) is calculated using relation (15) [35],

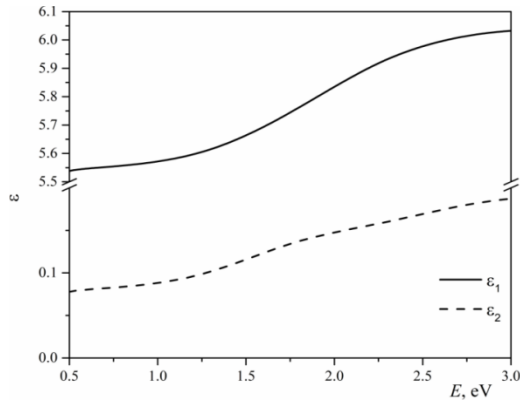


Fig. 7 – Real (ϵ_1) and imaginary (ϵ_2) parts of dielectric functions depending on photon energy of ZnO:Al thin film

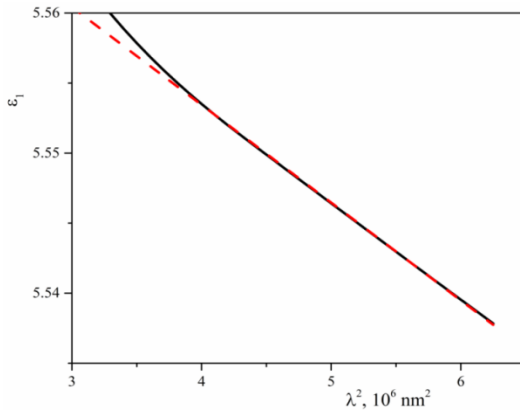


Fig. 8 – Variation of the real part of the dielectric coefficient (ϵ_1) with λ^2 for ZnO:Al thin film

$$\omega_p = \left(\frac{e^2 N_c}{\epsilon_0 m^*} \right)^{1/2}. \quad (15)$$

As expected, aluminium doping of ZnO thin films leads to an increase in ω_p value in comparison to pure ZnO (Table 3).

The dielectric loss factor $\tan\delta$ is determined by the known relation

$$\tan\delta = \frac{\epsilon_2}{\epsilon_1}, \quad (16)$$

and the corresponding photon energy dependence $\tan\delta(E)$ is presented in Fig. 9. The complex optical conductivity ($\sigma = \sigma_1 + i\sigma_2$) is known to be related to the complex dielectric constant (8) [29],

$$\sigma_1 = \omega\epsilon_2\epsilon_0, \quad \sigma_2 = \omega\epsilon_1\epsilon_0, \quad (17)$$

where ω is the angular frequency, ϵ_0 is the dielectric constant. Both components σ_1 and σ_2 of the optical conductivity σ increase with increasing frequency ω (Fig. 10).

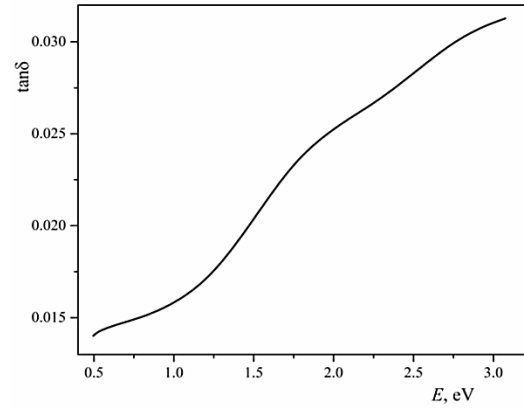


Fig. 9 – Variation of dielectric loss with energy for ZnO:Al thin film

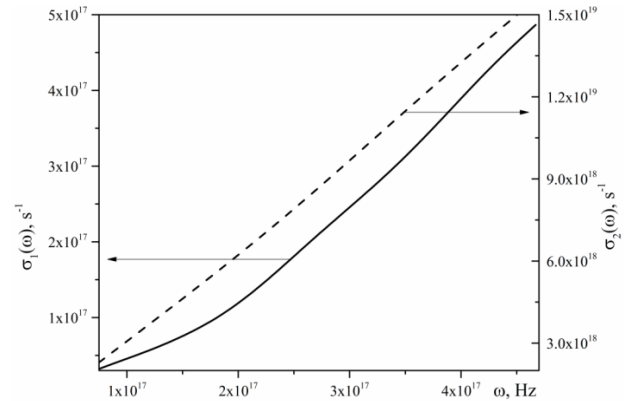


Fig. 10 – The optical conductivity dependence of frequency for ZnO:Al thin film

Table 3 – Optoelectronic constants of ZnO:Al thin films obtained from analysis of optical dielectric functions

Sample	Method of deposition	ϵ_∞	$\left(\frac{N_c}{m^*}\right)$, $\text{kg}^{-1} \text{m}^{-3}$	μ_{opt} , $\text{m}^2/\text{V s}$	ρ_{opt} , $\Omega^{-1} \text{m}^{-1}$	τ , s	ω_p , s^{-1}	Ref.
ZnO:Al	RF	5.48	$1.23 \cdot 10^{57}$	$6.7 \cdot 10^{-3}$	$3 \cdot 10^{-5}$	$1.68 \cdot 10^{-14}$	$6 \cdot 10^8$	This work
ZnO	Coating	2.993	$1.208 \cdot 10^{57}$	$3.643 \cdot 10^{-3}$	$3.544 \cdot 10^{-6}$	$0.913 \cdot 10^{-14}$	$5.720 \cdot 10^7$	[23]
ZnO:Fe-Ni (2 %)	Coating	3.562	$2.167 \cdot 10^{57}$	$5.095 \cdot 10^{-3}$	$1.412 \cdot 10^{-6}$	$1.276 \cdot 10^{-14}$	$8.620 \cdot 10^7$	[23]
ZnO	Sol-Gel	2.14	$2.11 \cdot 10^{56}$	–	–	–	–	[24]
ZnO:In (1.0 %)	Sol-Gel	2.71	$5.77 \cdot 10^{56}$	–	–	–	–	[24]

4. CONCLUSIONS

Optical characteristics of zinc oxide thin films with 2.5 wt. % aluminium content obtained by the RF method have been studied by the transmittance measurements in the wavelength spectral range of 300-2500 nm by the interferometry method. The data obtained have been used to calculate the complex dielectric function $\varepsilon = \varepsilon_1 + i\varepsilon_2$, complex refractive index $n = n_1 + in_2$ and several associated optical values of ZnO:Al thin films. The data obtained have been also elaborated using the Urbach approximation.

One of the main findings is the increase in Urbach energy for ZnO:Al thin films in comparison to the undoped ones. This probably is caused by an increase in the energy width of the localized electronic energy states of thin films due to increased atomic disorder. Also, an almost twofold increase in the optical oscillation

strength value has been revealed for the thin film studied.

Several electronic and optical parameters of the Drude free electron model (relaxation time, optical mobility and optical resistivity) for the thin films studied have been estimated for the first time. The doping of ZnO thin films with Al leads to an increase in the optical mobility, relaxation time and plasma frequency that was revealed by comparison with reference data for undoped ZnO.

Numerous optical parameters of ZnO:Al thin films obtained allow us to recommend these samples for applications in optoelectronic devices.

ACKNOWLEDGEMENTS

This work was supported by the Project of Young Scientists (No 0121U108649) of Ukraine.

REFERENCES

- V.M. Zhyrovetsky, D.I. Popovych, S.S. Savka, A.S. Serednytski, *Nanoscale Res. Lett.* **12**, 132 (2017).
- D.M. Bagnall, Y.F. Chen, M.Y. Shen, Z. Zhu, T. Goto, T. Yao, *J. Crystal Growth* **184-185**, 605 (1998).
- C.H. Ahn, Y.Y. Kim, S.W. Kang, H.K. Cho, *Physica B* **401-402**, 370 (2007).
- H.S. Kang, G.H. Kim, D.L. Kim, H.W. Chang, B.D. Ahn, S.Y. Lee, *Appl. Phys. Lett.* **89**, 181103 (2006).
- V.M. Latyshev, T.O. Berestok, A.S. Opanasyuk, A.S. Korniyushchenko, V.I. Perekrestov, *Solid State Sci.* **67**, 109 (2017).
- O. Dobrozhan, O. Diachenko, M. Kolesnyk, A. Stepanenko, S. Vorobiov, P. Baláz, S. Plotnikov, A. Opanasyuk, *Mater. Sci. Semicond. Proc.* **102**, 104595 (2019).
- R. Vittal, Kuo-Chuan Ho, *Renew. Sustain. Energy Rev.* **70**, 920 (2017).
- N. Bouchenak Khelladi, N.E. Chabane Sari, *Adv. Mater. Sci.* **13**, 21 (2013).
- A. Kashuba, H. Ilchuk, R. Petrus, I. Semkiv, O. Bovgyra, M. Kovalenko, V. Dzikovskiy, *Modern Phys. Lett. B* **35**, 2150189 (2021).
- V. Bilgina, E. Sarica, B. Demirsalcuk, K. Ertürk, *Physica B: Condens. Matter.* **599**, 412499 (2020).
- V. Romanyuk, N. Dmitruk, V. Karpyna, G. Lashkarev, V. Popovych, M. Dranchuk, R. Pietruszka, M. Godlewski, G. Dovbeshko, I. Timofeeva, O. Kondratenko, M. Taborska, A. Ievtushenko, *Acta Physica Polonica A* **129**, A-36 (2016).
- H.C.M. Knoop, van de B.W.H. Loo, S. Smit, M. Ponomarev, J.W. Weber, K. Sharma, W.M.M. Kessels, M. Creatore, *J. Vac. Sci. Technol. A* **33**, 021509 (2015).
- M.N. Amroun, K. Salim, A.H. Kacha, M. Khadraoui, *Int. J. Thin. Film. Sci. Tec.* **9**, 7 (2020).
- A.E. Youssef, M.H. Abd-El Salam, *Rad. Effect. Defect. Solids* **175**, 791 (2020).
- F.Z. Bedia, A. Bedia, N. Maloufi, M. Aillerie, *Adv. Struct. Mater.* **128**, 107 (2020).
- M.R. Islam, M.G. Azam, *Surf. Eng.* **37**, 775 (2020).
- X. Li, X. Zhu, K. Jin, D. Yang, *Opt. Mater.* **100**, 109657 (2020).
- Y. Aoun, R. Meneceur, S. Benramache, B. Maaoui, *Phys. Solid State* **62**, 131 (2020).
- L. Herissi, L. Hadjeris, M.S. Aida, S. Azizi, A. Hafdallah, A. Ferdi, *Nano Hybrid. Compos.* **27**, 21 (2019).
- M. Gabas, A. Landa-Cánovas, J.L. Costa-Krämer, F. Agulló-Rueda, A.R. González-Elipe, P. Díaz-Carrasco, J. Hernández-Moro, I. Lorite, P. Herrero, P. Castillero, A. Barranco, J.R. Ramos-Barrado, *J. Appl. Phys.* **113**, 163709 (2013).
- O. Bovgyra, M. Kovalenko, R. Bovhyra, V. Dzikovskiy, *J. Phys. Stud.* **23** No 4, 4301 (2019).
- V.B. Kapustianyk, B.I. Turko, V.P. Rudyk, B.Y. Kulyk, M.S. Rudko, *J. App. Spectr.* **82**, 153 (2015).
- A.M. Alsaad, A.A. Ahmad, Q.M. Al-Bataineh, A.A. Bani-Salameh, H.S. Abdullah, I.A. Qattan, Z.M. Albataineh, A.D. Telfah, *Materials* **13**, 1737 (2020).
- A. Kocyigit, M.O. Erdal, M. Yıldırım, *Zeitschrift für Naturforschung* **74**, 1 (2019).
- C. Manoharan, G. Pavithra, M. Bououdina, S. Dhanapandian, P. Dhamodharan, *Appl. Nanosci.* **6**, 815 (2016).
- H. Munawaroh, S. Wahyuningsih, A.H. Ramelan, *J. Nano-Electron. Phys.* **11**, 04028 (2019).
- M. Kovalenko, O. Bovgyra, V. Dzikovskiy, A. Kashuba, H. Ilchuk, R. Petrus, I. Semkiv, *Phys. Chem. Solid State* **22**, 153 (2021).
- F.Z. Bedia, A. Bedia, N. Maloufi, M. Aillerie, F. Genty, B. Benyoucef, *J. Alloy. Compd.* **616**, 312 (2014).
- Y. Caglar, S. Ilican, M. Caglar, *Eur. Phys. J. B* **58**, 251 (2007).
- I.S. Yahia, A.A.M. Farag, M. Cavas, F. Yakuphanoglu, *Superlattice. Microst.* **53**, 63 (2013).
- H. Ilchuk, R. Petrus, A. Kashuba, I. Semkiv, E. Zmiovska, *Molec. Cryst. Liq. Cryst.* **699**, 1 (2020).
- L.I. Nykyruy, R.S. Yavorskyi, Z.R. Zapukhlyak, G. Wisz, P. Potera, *Opt. Mater.* **92**, 319 (2019).
- C.E. Benouis, M. Benhaliliba, A.S. Juarez, M.S. Aida, F. Chami, F. Yakuphanoglu, *J. Alloy. Compd.* **490**, 62 (2010).
- A.Y. Fasasi, E. Osagie, D. Pelemo, E. Obiajunwa, E. Ajenifuja, J. Ajao, G. Osinkolu, W.O. Makinde, A.E. Adeoye, *Am. J. Mater. Synth. Process.* **3**, 12 (2018).
- F. Yakuphanoglu, M. Sekerci, *J. Molec. Struct.* **751**, 200 (2005).

Оптичні та дисперсійні параметри тонких плівок ZnO:AlА.І. Кашуба¹, Б. Андрієвський², Г.А. Ільчук¹, Р.Ю. Петрусь¹, Т.С. Малій³, І.В. Семків¹¹ Національний університет «Львівська політехніка», вул. С. Бандери, 12, 79646 Львів, Україна² Факультет електроніки та комп'ютерних наук, Кошалінський технологічний університет, 75-453 Кошалін, Польща³ Львівський національний університет імені Івана Франка, вул. Кирила і Мефодія, 8, 79005 Львів, Україна

Представлені результати досліджень дисперсії параметрів та оптичних функцій для тонкої плівки оксиду цинку, легованої алюмінієм. Осадження тонких плівок ZnO, легованих Al (2,5 мас. %), виконувалось методом височастотного магнетронного напилення. Тонка плівка ZnO:Al кристалізується в гексагональній структурі (тип структури ZnO, просторова група $R\bar{6}_3mc$ (No. 186), з параметрами елементарної комірки $a = 3.226(2) \text{ \AA}$ і $c = 5.155(6) \text{ \AA}$ ($V = 46.49(6) \text{ \AA}^3$). Спектри оптичного пропускання (300-2500 нм) показали, що тонка плівка ZnO:Al має високу оптичну якість, а значення величини оптичної ширини забороненої зони (3,26 eV) є дуже близьким до нелегованих зразків. Встановлено спектральну поведінку оптичних функцій: показника заломлення, коефіцієнта екстинкції, показника поглинання, діелектричних функцій та оптичної провідності. Встановлено значення енергії Урбаха та залежність сили осцилятора від оптичної ширини забороненої зони та концентрації легуючого елемента. Спостерігається збільшення енергії Урбаха для легованої Al тонкої плівки ZnO порівняно з нелегованою. Для досліджуваної тонкої плівки виявлено майже подвійне збільшення значення сили оптичного осцилятора в порівнянні із нелегованими зразками. Вплив легування алюмінієм тонких плівок ZnO на динаміку зміни оптичної рухливості, оптичного опору та часу релаксації встановлено вперше для досліджуваної сполуки. Також, визначається значення плазмової частоти та її кореляція з концентрацією носіїв. Легування тонких плівок ZnO алюмінієм призводить до збільшення оптичної рухливості, часу релаксації та плазмової частоти, що було виявлено порівнянням з відомими даними для нелегованих тонких плівок ZnO. Виявлені оптичні властивості досліджуваної тонкої плівки вказують на перспективи її практичного використання як матеріалу для оптоелектронних пристроїв.

Ключові слова: Тонкі плівки, Поглинання, Дисперсія, Показник заломлення, Пропускання, Оптичні функції, Час релаксації.